

Headline Articles

Insertion of Phenylacetylene into [Pt(GeMe$_3$)(SnMe$_3$)(PMe$_2$Ph)$_2$]

Takashi Sagawa,[1] Rika Tanaka,[1] and Fumiyuki Ozawa*

International Research Center for Elements Science, Institute for Chemical Research, Kyoto University, Uji, Kyoto 611-0011

[1]Department of Applied Chemistry, Graduate School of Engineering, Osaka City University, Sumiyoshi-ku, Osaka 558-8585

Received February 3, 2004; E-mail: ozawa@scl.kyoto-u.ac.jp

The reaction of $Me_3GeSnMe_3$ with a platinum(0) complex, in situ generated from [Pt(cod)$_2$] (cod = 1,5-cyclooctadiene) and 2 molar quantity of PMe_2Ph in Et_2O, formed a cis–trans mixture of [Pt(GeMe$_3$)(SnMe$_3$)(PMe$_2$Ph)$_2$] (**1**). Recrystallization of crude **1** from CH_2Cl_2–pentane gave pure *cis*-**1**, while the isolated cis isomer was again converted to an equilibrium mixture (cis:trans = 8:2) in solution. The cis–trans mixture of **1** underwent competitive insertion of phenylacetylene into Pt–Sn and Pt–Ge bonds to give *cis*-[Pt(GeMe$_3$){C(Ph)=CH(SnMe$_3$)}(PMe$_2$Ph)$_2$] (**2a**) and *cis*-[Pt{C(Ph)=CH(GeMe$_3$)}(SnMe$_3$)(PMe$_2$Ph)$_2$] (**3a**), respectively, in a ratio of 80:20, while **2a** was thermodynamically less stable, and converted to **3a** in solution. The insertion mechanism was examined by kinetic investigations.

Complexes bearing inter-element linkages between group 10 metals and heavy group 14 elements have attracted a great deal of interest.[1] This is not only due to their key roles in the catalytic addition of element–element bonds to unsaturated hydrocarbons, but also due to their unique structures and chemical properties, significantly different from those of common organometallic complexes with metal–carbon and metal–hydrogen bonds.[2–9] For example, *cis*-[M(ER$_3$)(E′R$_3$)L$_2$] complexes (M = Pd, Pt; ER$_3$, E′R$_3$ = silyl, germyl, stannyl; L = tertiary phosphine) have a twisted structure significantly distorted from a square planar geometry, which is rather unusual for complexes having a d^8 metal center.[5,6,7a–d] Furthermore, it has been documented that these complexes undergo rapid twist-rotation via a tetrahedral transition state in solution (Scheme 1).[5]

We are currently interested in the reaction chemistry of such complexes, particularly in alkyne-insertion into metal–element bonds and reductive elimination giving carbon–element bonds.[7,8] Although these reactions have been assumed to be key elementary processes for catalytic reactions,[1] their details, especially from mechanistic viewpoints, have remained nearly unexplored. In this paper, we describe the synthesis and alkyne-insertion reaction of [Pt(GeMe$_3$)(SnMe$_3$)(PMe$_2$Ph)$_2$] (**1**).[10] This study is closely related to our previous report on *cis*-[Pt(SiR$_3$)(SnMe$_3$)L$_2$] complexes (**A**) (SiR$_3$ = SiMe$_3$, SiMe$_2$Ph, SiMePh$_2$, SiPh$_3$).[7b,c] Thus, we performed kinetic investigations on the insertion of alkynes (ArC≡CH) into **A** in solution, and confirmed the following points: (i) **A** undergoes the competitive insertion of alkynes into Pt–Sn and Pt–Si bonds to give *cis*-[Pt(SiR$_3$){C(Ar)=CH(SnMe$_3$)}L$_2$] (**B**) and *cis*-[Pt{C(Ar)=CH(SiR$_3$)}(SnMe$_3$)L$_2$] (**C**), respectively. (ii) Although **B** is further isomerized to **C** in solution, this reaction is effectively suppressed by the addition of free L to the system. Accordingly, we could observe the ratio of competitive insertion into the Pt–Sn and Pt–Si bonds under a kinetic condition as well as the ratio of **B** to **C** under a thermodynamic condition by choosing the presence or absence of added L. (iii) The kinetic ratio of **B** to **C** in the competitive insertion markedly varies with silyl ligands [e.g., **B**:**C** = 0:100 (SiMe$_3$), 30:70 (SiMe$_2$Ph), 59:41 (SiMePh$_2$), 97:3 (SiPh$_3$), for PhC≡CH (alkyne) and PMe$_2$Ph (L)]. On the other hand, (iv) **C** is thermodynamically more stable than **B** irrespective of the silyl ligands.

As described below, germyl(stannyl) complex **1** behaves very similarly to silyl(stannyl) complexes **A**. Thus, **1** undergoes competitive insertion of phenylacetylene into Pt–Ge and Pt–Sn bonds under kinetic conditions, whereas under thermodynamic conditions, the complex derived from the insertion into Pt–Sn bond is exclusively converted to the other complex formed

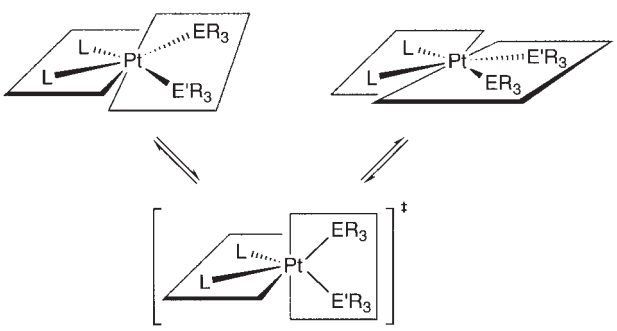

Scheme 1.

Published on the web July 9, 2004; DOI 10.1246/bcsj.77.1287

by insertion into the Pt–Ge bond.

Results and Discussion

Synthesis of [Pt(GeMe$_3$)(SnMe$_3$)(PMe$_2$Ph)$_2$] (1). The treatment of [Pt(cod)$_2$] with PMe$_2$Ph (2 molar quantity) and Me$_3$GeSnMe$_3$ (1 molar quantity) in Et$_2$O at room temperature gave a yellow solution containing cis and trans isomers of [Pt(GeMe$_3$)(SnMe$_3$)(PMe$_2$Ph)$_2$] (**1**) in an 8:2 ratio, as confirmed by ^{31}P{^{1}H} NMR spectroscopy (Scheme 2). Concentration of the solution by pumping, followed by washing the resulting precipitate with pentane, afforded a yellow solid of *cis*-**1** in 73% yield, which was further purified by recrystallization from CH$_2$Cl$_2$/pentane to give single crystals of *cis*-**1** (56%), suitable for X-ray diffraction analysis.

Figure 1 shows an ORTEP diagram of *cis*-**1**, which adopts a twisted structure significantly distorted from the square planar geometry around platinum. The dihedral angle between the PtP(1)P(2) and PtGeSn planes is 31.3°, and the Pt–Ge and Pt–Sn bonds are tilted from the PtP$_2$ plane by 19.9 and 21.0°, respectively, toward opposite directions from each other.

The isolated *cis*-**1** underwent cis–trans isomerization in CD$_2$Cl$_2$ at 20 °C to give an equilibrium mixture containing an 80:20 ratio of cis and trans isomers in 3 h. The isomerization

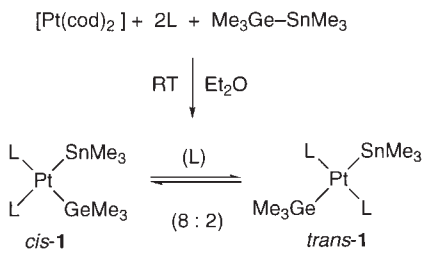

Scheme 2. L = PMe$_2$Ph.

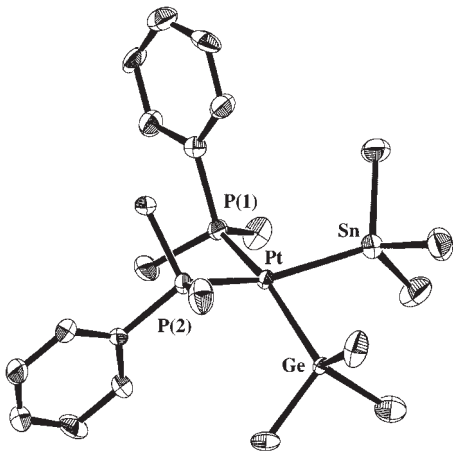

Fig. 1. X-ray structure of *cis*-**1**. The thermal ellipsoids are drawn at 50% probability levels. Hydrogen atoms are omitted for clarity. Selected bond distances (Å) and angles (deg): Pt–Ge = 2.511(1), Pt–Sn = 2.580(1), Pt–P(1) = 2.310(3), Pt–P(2) = 2.315(3), Ge–Pt–Sn = 84.60(4), Ge–Pt–P(1) = 157.32(8), Ge–Pt–P(2) = 93.27(8), Sn–Pt–P(1) = 92.92(8), Sn–Pt–P(2) = 156.53(8), P(1)–Pt–P(2) = 97.6(1).

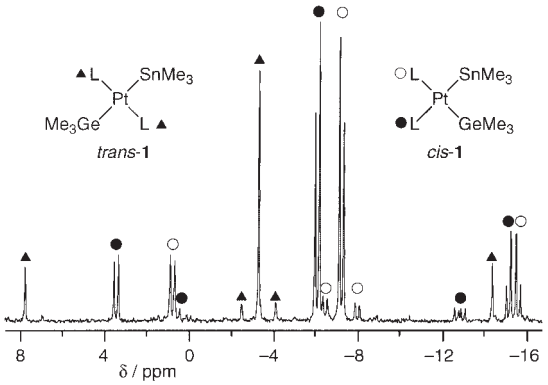

Fig. 2. ^{31}P{^{1}H} NMR spectrum of a mixture of *cis*- and *trans*-**1** in CD$_2$Cl$_2$ at −50 °C (121.49 MHz). L = PMe$_2$Ph.

was markedly accelerated by the addition of free PMe$_2$Ph to the system. Thus, equilibrium was established within a few minutes in CD$_2$Cl$_2$ at 20 °C in the presence of a 0.1 molar quantity of PMe$_2$Ph. This observation is consistent with the Berry's pseudo-rotation process involving five-coordinate intermediates generated by the coordination of PMe$_2$Ph to **1**. A similar isomerization process has been proposed for bis(germyl)platinum complexes.[3,6]

The cis and trans geometries of **1** in solution were confirmed by ^{31}P{^{1}H} NMR spectroscopy. Figure 2 shows the ^{31}P{^{1}H} NMR spectrum of an equilibrium mixture of **1** in CD$_2$Cl$_2$ at −50 °C. The two sets of doublets at δ −5.9 and −7.1 are ascribed to *cis*-**1**, and the singlet at δ −3.2 to *trans*-**1**. The latter involves ^{195}Pt satellites with the $^1J_{PtP}$ coupling constant of 2691 Hz. This value is consistent with the trans arrangement of two phosphorus atoms around platinum. On the other hand, the doublet signals at δ −5.9 and −7.1 for *cis*-**1** exhibit the $^1J_{PtP}$ values of 2309 and 1940 Hz, respectively; the values are consistent with the *cis*-PtP$_2$ structure having stannyl and germyl ligands trans to the phosphine ligands, respectively. Since the doublet at δ −5.9 involves large couplings to Sn [1686 (^{119}Sn), 1612 (^{117}Sn)] whereas the doublet at δ −7.1 involves relatively small couplings [189 (^{119}Sn), 181 (^{117}Sn)], the former and latter signals are assignable to the phosphorus trans and cis to the SnMe$_3$ ligand, respectively.

The signal of *trans*-**1** was temperature-independent. On the other hand, the two sets of doublets of *cis*-**1** gradually broadened at elevated temperatures, and coalesced into a broad doublet at 37 °C. A similar behavior has been observed for related bis(silyl)-,[7d] silyl(stannyl)-,[7b,c] and bis(stannyl)platinum(II)[5] complexes, and attributed to the occurrence of a rapid twist-rotation via a tetrahedral transition state (Scheme 1).[5] In the present case, the rate of rotation was estimated to be 1.8(2) × 10 s^{-1} at 20 °C by applying the chemical shifts of the main peaks to the Gutowsky–Holm's equation.[11]

Alkyne-Insertion. We have confirmed that germyl(stannyl) complex **1** undergoes two types of processes in solution: cis–trans isomerization and twist-rotation. The latter is operative on an NMR time-scale. On the other hand, the former is a relatively slow process, but notably accelerated by added PMe$_2$Ph. Having these observations in hand, we next examined alkyne-insertion into **1**.

Complex **1** (25 mM) was treated with phenylacetylene (0.25

M) in CD_2Cl_2 at 20 °C. As can be seen from the time-course given in Fig. 3a, the cis and trans isomers of **1** were simultaneously reduced to be replaced by *cis*-[Pt{C(Ph)=CH($GeMe_3$)}($SnMe_3$)(PMe_2Ph)$_2$] (**3a**). Thus, the initial ratio of the two geometrical isomers of **1** (cis:trans = 81:19) was almost unchanged during the reaction. The formation of **3a** obeyed pseudo-first-order kinetics with respect to the total concentration of *cis*- and *trans*-**1** ($k_{obsd} = 1.55(2) \times 10^{-3}$ s^{-1}).

On the other hand, when the reaction was carried out in the presence of added PMe_2Ph (9 mM), *cis*-[Pt($GeMe_3$){C(Ph)=CH($SnMe_3$)}(PMe_2Ph)$_2$] (**2a**) was observed in addition to **3a** (Fig. 3b). Similarly to the reaction without added PMe_2Ph, the initial isomer ratio of **1** (cis:trans = 78:22) remained almost constant throughout the reaction. Furthermore, the ratio of **2a** to **3a** (80:20) remained constant ($k_{obsd} = 0.92(2) \times 10^{-3}$ s^{-1}).

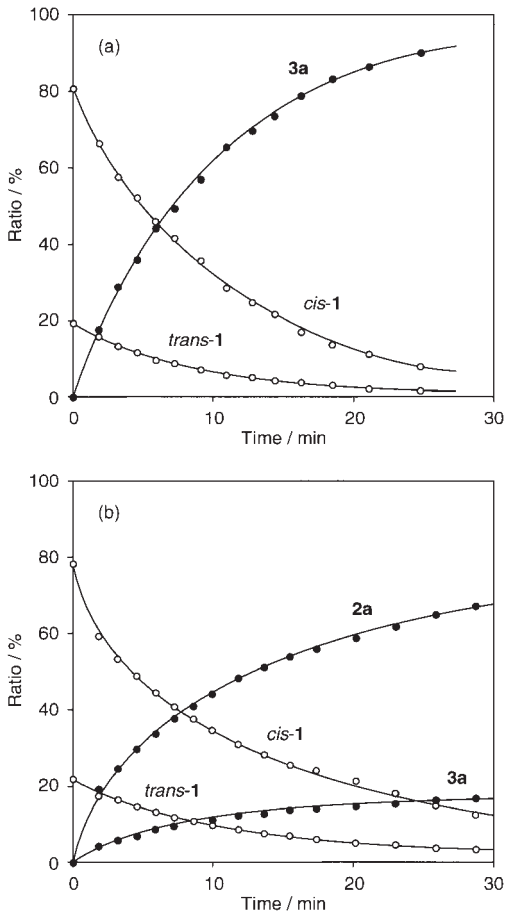

Fig. 3. Time-courses of the reaction of **1** with phenylacetylene in CD_2Cl_2 in the absence (a) and presence (b) of added PMe_2Ph at 20 °C. Initial concentration: [**1**] = 25 mM, [PhC≡CH] = 0.25 M, [PMe_2Ph] = 0 (a) or 9 mM (b).

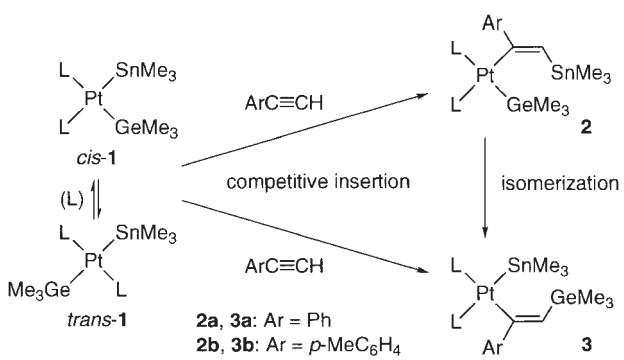

Scheme 3. L = PMe_2Ph.

The site of phenylacetylene-insertion (i.e., Pt–Ge or Pt–Sn) was found to be altered by the absence or presence of added PMe_2Ph. As described in the introductory part, almost the same dependence of the insertion site on the amount of added phosphine was observed for *cis*-[Pt(SiR_3)($SnMe_3$)L_2] complexes (**A**).[7b,c] We may therefore consider very similar reaction processes for the present germyl(stannyl) complex **1** as well (Scheme 3). Thus, **1** undergoes competitive insertion of phenylacetylene into the Pt–Sn and Pt–Ge bonds to give the insertion complexes **2a** and **3a**, respectively. Since **2a** is thermodynamically less stable than **3a**, this complex may be successively converted to **3a**. Accordingly, **3a** was observed as the sole insertion product in the absence of added PMe_2Ph (Fig. 3a). However, since the isomerization is effectively retarded by free PMe_2Ph, the kinetic ratio of **2a** to **3a** (80:20) in the competitive insertion is preserved in the presence of added PMe_2Ph. Actually, a kinetic mixture of **2a** and **3a**, generated from **1** (25 mM) and phenylacetylene (0.25 M) in toluene-d_8 in the presence of added PMe_2Ph (5 mM) at 20 °C, was totally converted to **3a** in 12 h upon heating (50 °C).

Figure 4 shows the $^{31}P\{^1H\}$ NMR spectra of **2a** (a) and **3a** (b). Two sets of doublets with Pt and Sn satellites can be observed for each complex. The signals of **3a** involve J_{SnP} couplings comparable to *cis*-**1** [1789 (^{119}Sn) and 1710 (^{117}Sn) Hz for δ −13.8; 168 (^{119}Sn) and 160 (^{117}Sn) Hz for δ −16.0]. This

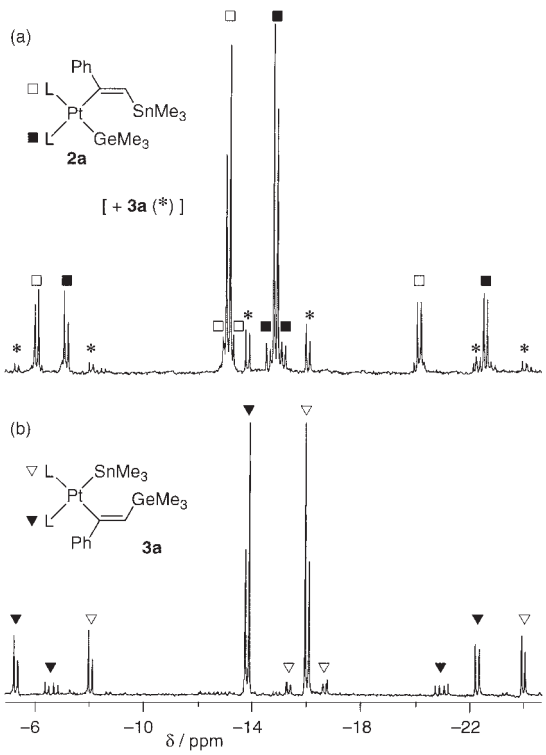

Fig. 4. $^{31}P\{^1H\}$ NMR spectra of **2a** (a) and **3a** (b) in CD_2Cl_2 at 20 °C (121.49 MHz). The sample of (a) contains a small amount to **3a**. L = PMe_2Ph.

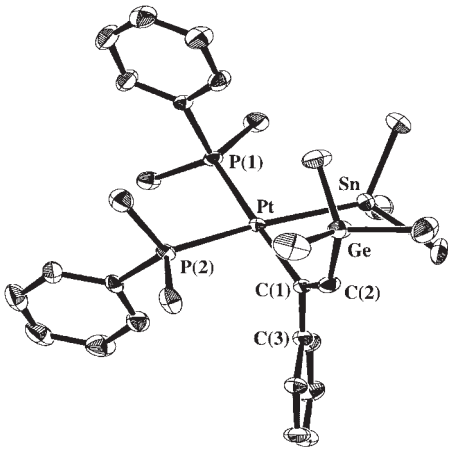

Fig. 5. X-ray structure of **3a**. The thermal ellipsoids are drawn at 30% probability levels. Hydrogen atoms are omitted for clarity. Selected bond distances (Å) and angles (deg): Pt–Sn = 2.6140(7), Pt–P(1) = 2.301(2), Pt–P(2) = 2.338(2), Pt–C(1) = 2.090(6), C(1)–C(2) = 1.325(7), C(1)–C(3) = 1.501(9), Ge–C(2) = 1.930(7), Sn–Pt–P(1) = 92.38(5), Sn–Pt–P(2) = 173.54(4), Sn–Pt–C(1) = 84.0(2), P(1)–Pt–P(2) = 94.07(6), P(1)–Pt–C(1) = 175.4(2), P(2)–Pt–C(1) = 89.6(2), Pt–C(1)–C(2) = 127.9(5), Pt–C(1)–C(3) = 114.8(3), C(2)–C(1)–C(3) = 117.3(5), Ge–C(2)–C(1) = 133.3(5).

fact is consistent with the presence of a Pt–Sn bond in **3a**. On the other hand, the J_{SnP} couplings observed for **2a** were small [29 Hz for δ −13.1; 68 Hz for δ −14.9].

The regiochemistry of phenylacetylene-insertion giving the structures "PtC(Ph)=CH($SnMe_3$)" in **2a** and "PtC(Ph)=CH($GeMe_3$)" in **3a** was determined by $^{13}C\{^1H\}$ NMR spectroscopy. Thus, the α-vinylic carbon bonded to platinum appeared as a doublet of doublets with ^{195}Pt satellites, respectively [**2a**: δ 179.4 (dd, $^2J_{PC}$ = 103 and 14 Hz, $^1J_{PtP}$ = 749 Hz); **3a**: δ 172.7 (dd, $^2J_{PC}$ = 100 and 13 Hz, $^1J_{PtC}$ = 704 Hz)]. Since these signals disappeared in the DEPT NMR spectra, they were assigned to the phenyl-substituted carbons.

The structure of **3a** was further confirmed by X-ray diffraction analysis. The ORTEP diagram given in Fig. 5 shows a square planar structure having $SnMe_3$ and C(Ph)=CH($GeMe_3$) ligands in mutually cis positions. The $GeMe_3$ group is oriented cis and trans to the platinum and phenyl group, respectively, showing the occurrence of cis insertion of phenylacetylene into the Pt–Ge bond.

The insertion reactions were examined with other alkynes. The reaction of **1** (25 mM) with *p*-$MeC_6H_4C{\equiv}CH$ (0.25 M) in CD_2Cl_2 in the presence of added PMe_2Ph (9 mM) proceeded with a pseudo-first-order rate constant of $7.00(5) \times 10^{-4}$ s^{-1} at 20 °C to give **2b** and **3b** in a 78:22 ratio (Scheme 3). On the other hand, **1** (25 mM) reacted with $MeO_2CC{\equiv}CCO_2Me$ (25 mM) instantly at room temperature to afford *cis*-[Pt($GeMe_3$)-{C(CO_2Me)=C(CO_2Me)($SnMe_3$)}(PMe_2Ph)$_2$] (**2c**) as the insertion product into Pt–Sn bond, selectively.

Kinetic Study. The competitive insertion in the presence of added PMe_2Ph was examined by kinetic experiments. Table 1 lists the pseudo-first-order rate constants measured under various concentrations of PhC≡CH and PMe_2Ph. The product ratio

Table 1. Pseudo-First-Order Rate Constants for the Insertion of Phenylacetylene into **1**[a)]

Run	[PhC≡CH]/M	[PMe_2Ph]/mM	$10^3k_{obsd}/s^{-1}$
1	0.25	9	0.92(2)
2	0.25	23	0.759(2)
3	0.25	36	0.49(1)
4	0.25	60	0.349(7)
5	0.16	23	0.45(1)
6	0.45	23	1.31(1)
7	0.64	23	1.87(4)

a) All runs were carried out in CD_2Cl_2 at 20 °C. Initial concentration: $[\mathbf{1}]_0$ = 25 mM.

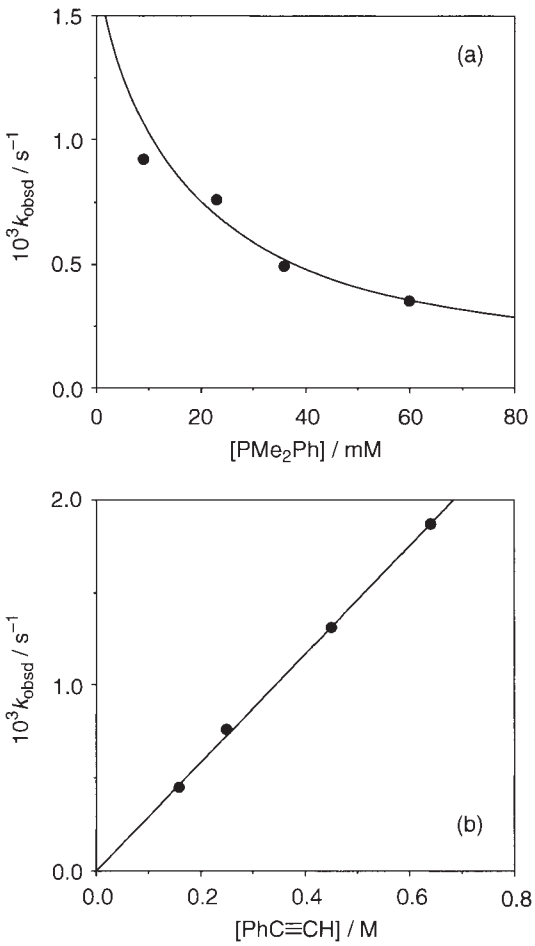

Fig. 6. (a) Plot of pseudo-first-order rate-constants against the concentration of added PMe_2Ph for the data of runs 1–4 in Table 1. The curve line is based on Eq. 8. (b) Plot of pseudo-first-order rate-constants against phenylacetylene-concentration for the data of runs 2 and 5–7 in Table 1. The straight line is based on least-squares calculation.

of **2a** to **3a** was 80:20 for all runs. Furthermore, the equilibrium between *cis*- and *trans*-**1** was established through the reactions. The reaction progress was retarded by added PMe_2Ph (runs 1–4; Fig. 6a). On the other hand, the reaction rate increased linearly as the concentration of phenylacetylene increased (runs 2 and 5–7; Fig. 6b).

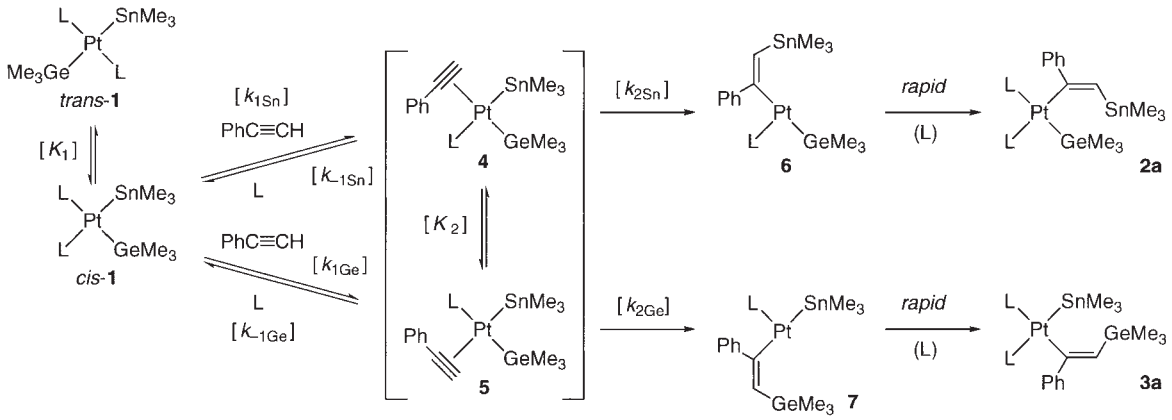

Scheme 4. L = PMe_2Ph.

These kinetic observations are in good accordance with those previously reported for *cis*-silyl(stannyl)platinum complexes (**A**).[7b] Accordingly, we may assume a very similar insertion mechanism, as depicted in Scheme 4. The only difference is the occurrence of cis–trans isomerization of the starting **1**. Thus, unlike the silyl(stannyl) complexes, for which only cis isomers are present, we must consider which isomer of **1** is reactive toward the insertion. Although we could obtain no direct information concerning this point, a previous observation on a related insertion system may be taken as an indication that *cis*-**1** is the active species. Thus, it has been confirmed that only the cis isomer of $[PtMe(SiPh_3)(PMe_2Ph)_2]$ undergoes the insertion of phenylacetylene, whereas the trans isomer is totally inactive toward insertion.[7e,f]

The next step is the coordination of phenylacetylene with *cis*-**1**. This step is considered to proceed via an associative displacement of one of the PMe_2Ph ligands (L) with phenylacetylene. The presence of partial dissociation of L, prior to rate-determining insertion, is in agreement with the fact that the insertion is retarded by the addition of L to the system (Fig. 6a). Complexes **4** and **5** thus formed are very probably interconverted with each other by twist-rotation, as observed for *cis*-**1**. These intermediates then undergo migratory insertion of the coordinated acetylene into the Pt–Sn or Pt–Ge bond. The resulting **6** and **7** are further converted to **2a** and **3a**, respectively, by trans to cis isomerization, followed by the coordination of L.

When the interconversion between **4** and **5** is rapid enough to keep the ratio of **4** to **5** constant, and the steady-state approximation can be applied to the total concentration of **4** and **5**, the following relation holds:

$$(k_{1Sn} + k_{1Ge})[PhC{\equiv}CH][cis\text{-}\mathbf{1}] = (k_{-1Sn}[\mathbf{4}] + k_{-1Ge}[\mathbf{5}])[L] + (k_{2Sn}[\mathbf{4}] + k_{2Ge}[\mathbf{5}]). \quad (1)$$

Since $[\mathbf{5}] = K_2[\mathbf{4}]$,

$$(k_{1Sn} + k_{1Ge})[PhC{\equiv}CH][cis\text{-}\mathbf{1}] = \{(k_{-1Sn} + k_{-1Ge}K_2)[L] + (k_{2Sn} + k_{2Ge}K_2)\}[\mathbf{4}]. \quad (2)$$

Accordingly,

$$[\mathbf{4}] = \frac{(k_{1Sn} + k_{1Ge})[PhC{\equiv}CH]}{(k_{-1Sn} + k_{-1Ge}K_2)[L] + (k_{2Sn} + k_{2Ge}K_2)}[cis\text{-}\mathbf{1}]. \quad (3)$$

On the other hand, if the conversions of **6** to **2a** and **7** to **3a** are sufficiently faster than the migratory insertion in **4** and **5**, the sum of the formation rates of **2a** and **3a** can be expressed as follows:

$$\frac{d[\mathbf{2a}]}{dt} + \frac{d[\mathbf{3a}]}{dt} = k_{2Sn}[\mathbf{4}] + k_{2Ge}[\mathbf{5}] = (k_{2Sn} + k_{2Ge}K_2)[\mathbf{4}]. \quad (4)$$

Substitution of Eq. 3 into Eq. 4 yields the following rate expression:

$$\frac{d[\mathbf{2a}]}{dt} + \frac{d[\mathbf{3a}]}{dt} = \frac{(k_{1Sn} + k_{1Ge})(k_{2Sn} + k_{2Ge}K_2)[PhC{\equiv}CH]}{(k_{-1Sn} + k_{-1Ge}K_2)[L] + (k_{2Sn} + k_{2Ge}K_2)}[cis\text{-}\mathbf{1}] = (k_{obsd}[\mathbf{1}]). \quad (5)$$

Since $[\mathbf{1}] = [cis\text{-}\mathbf{1}] + [trans\text{-}\mathbf{1}]$ and $[cis\text{-}\mathbf{1}]/[trans\text{-}\mathbf{1}] = K_1$,

$$[cis\text{-}\mathbf{1}] = \frac{K_1}{1 + K_1}[\mathbf{1}]. \quad (6)$$

Therefore, the rate expressions given below are obtained:

$$-\frac{d[\mathbf{1}]}{dt} = k_{obsd}[\mathbf{1}] = \frac{K_1}{(1 + K_1)} \times \frac{(k_{1Sn} + k_{1Ge})(k_{2Sn} + k_{2Ge}K_2)[PhC{\equiv}CH]}{(k_{-1Sn} + k_{-1Ge}K_2)[L] + (k_{2Sn} + k_{2Ge}K_2)}[\mathbf{1}], \quad (7)$$

$$\frac{K_1[PhC{\equiv}CH]}{(1 + K_1)k_{obsd}} = \frac{(k_{-1Sn} + k_{-1Ge}K_2)[L]}{(k_{1Sn} + k_{1Ge})(k_{2Sn} + k_{2Ge}K_2)} + \frac{1}{(k_{1Sn} + k_{1Ge})}. \quad (8)$$

Figure 7 shows a plot of the $K_1[PhC{\equiv}CH]_0/(1 + K_1)k_{obsd}$ values against the $[PMe_2Ph]$ values for all runs listed in Table 1, giving a good linear correlation ($r = 0.985$), consistent with Eq. 8. Based on the intercept and slope, the $(k_{1Sn} + k_{1Ge})$ and $(k_{-1Sn} + k_{-1Ge}K_2)/(k_{2Sn} + k_{2Ge}K_2)$ values were estimated to be 0.86×10^{-2} s^{-1} M^{-1} and 65, respectively.

Finally, the conversion of **2a** to **3a** was confirmed to be operative by an intramolecular process. Thus, no incorporation of *p*-$MeC_6H_4C{\equiv}CH$ into **3** was observed, when a kinetic mixture of **2a** and **3a** in an 80:20 ratio was heated with 3 molar quantity of *p*-$MeC_6H_4C{\equiv}CH$ in toluene-d_8 at 50 °C (Scheme 5). Similarly, heating a mixture of **2b** and **3b** (78:22) with PhC≡CH (3 molar quantity) in toluene-d_8 at 50 °C for 12 h led to the selective formation of **3b**.

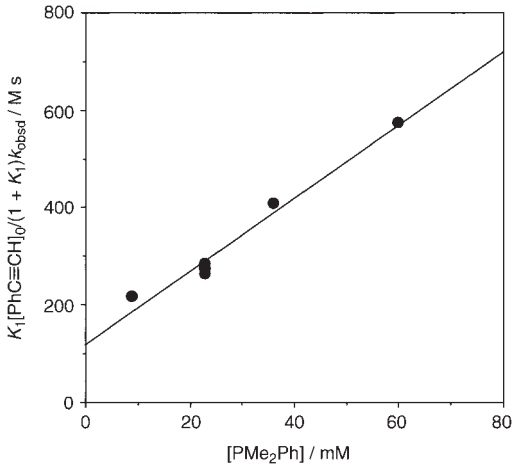

Fig. 7. Plot of $K_1[PhC{\equiv}CH]/(1 + K_1)k_{obsd}$ values against the concentration of added PMe_2Ph for all data in Table 1. The straight line is based on least-squares calculation.

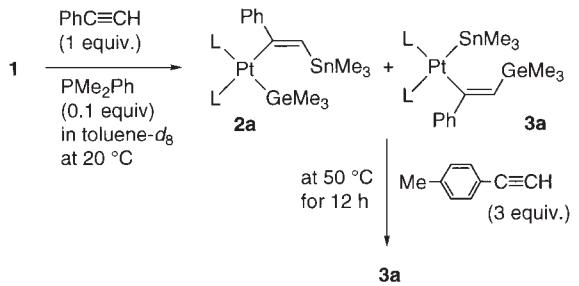

Scheme 5. L = PMe_2Ph.

Comparison of the Reactivities of Platinum–Element Bonds. We have studied phenylacetylene-insertion into [$Pt(GeMe_3)(SnMe_3)(PMe_2Ph)_2$] (**1**). While **1** undergoes cis–trans isomerization, the essential features of the insertion were very similar to those observed for *cis*-silyl(stannyl)platinum complexes (**A**). Therefore, we now have data to compare the relative reactivities of the platinum–group 14 element bonds toward phenylacetylene-insertion. Table 2 lists the site-selectivities observed for [$Pt(EMe_3)(E'Me_3)(PMe_2Ph)_2$] type complexes under kinetic and thermodynamic conditions. The site-selectivities measured under kinetic conditions suggest the following reactivity order: Pt–$SiMe_3$ > Pt–$SnMe_3$ > Pt–$GeMe_3$. This order seems to reflect a balance of the strength of Pt–element and C–element bonds, which are cleaved and formed upon insertion, respectively. Thus, the bond dissociation energies of the Pt–element bonds decrease in the order (in kJ mol^{-1}): Pt–$SiMe_3$ (233) > Pt–$GeMe_3$ (182) > Pt–$SnMe_3$ (172),[12] whereas those of C–element bonds decrease in the order: Me–Si (317) > Me–Ge (265) > Me–Sn (226); Et–Si (287) > Et–Ge (243) > Et–Sn (195); Ph–Si (358) > Ph-Ge (312) > Ph–Sn (261).[13] On the other hand, the insertion site under thermodynamic conditions seems to simply reflect the strength of the C–element bonds (i.e., Pt–$SiMe_3$ > Pt–$SnMe_3$ and Pt–$GeMe_3$ > Pt–$SnMe_3$), though direct information about the site-selectivity between Pt–Si and Pt–Ge bonds is presently unavailable.[14]

Experimental

General Considerations. All manipulations were carried out under a nitrogen atmosphere using conventional Schlenk techniques. Nitrogen gas was dried by passing through P_2O_5 (Merck, SICAPENT). NMR spectra were recorded on a Varian Mercury 300 spectrometer. Chemical shifts are reported in δ (ppm), referenced to the ^1H (of residual protons) and ^{13}C signals of the deuterated solvents, or to the ^{31}P signal of external 85% H_3PO_4 standard. Elemental analysis was performed on a Perkin-Elmer 2400II CHN Analyzer. Et_2O, pentane, and toluene-d_8 were dried over sodium diphenylketyl and distilled prior to use. CH_2Cl_2 was dried over CaH_2 and distilled prior to use. CD_2Cl_2 was dried over $LiAlH_4$, vacuum transferred, and stored under a nitrogen atmosphere. [$Pt(cod)_2$] was prepared according to literature.[15] All other chemicals were obtained from commercial suppliers and used without purification.

Preparation of *cis*-[$Pt(GeMe_3)(SnMe_3)(PMe_2Ph)_2$] (1). To a white suspension of [$Pt(cod)_2$] (207 mg, 0.50 mmol) in Et_2O (10 mL) were successively added PMe_2Ph (139 mg, 1.0 mmol) and $Me_3GeSnMe_3$ (142 mg, 0.50 mmol) at room temperature. The mixture was stirred for 10 min to give a yellow homogeneous solution. $^{31}P\{^1H\}$ NMR analysis of the solution revealed the formation of *cis*- and *trans*-**1** in an 8:2 ratio. The solvent was removed by pumping, and the resulting oily material was cooled to -78 °C and dissolved in Et_2O (1 mL). The slow addition of pentane (3 mL) with vigorous stirring led to the precipitation of a pale yellow solid of **1**, which was collected by filtration, washed with pentane (2 mL × 2), and dried under vacuum (275 mg, 73%). Recrystallization of the crude product from CH_2Cl_2/pentane gave analytically pure *cis*-**1** as yellow crystals (211 mg, 56%).

***cis*-1**. ^1H NMR (CD_2Cl_2, -50 °C) δ -0.02 (s, $^3J_{PtH} = 9.0$ Hz, $^2J_{SnH} = 36.6$ Hz, 9H, SnMe), 0.24 (d, $^4J_{PH} = 2.1$ Hz, $^3J_{PtH} = 15.6$ Hz, 9H, GeMe), 1.56 (d, $^2J_{PH} = 8.1$ Hz, $^3J_{PtH} = 25.8$ Hz, 6H, PMe), 1.57 (d, $^2J_{PH} = 7.8$ Hz, $^3J_{PtH} = 24.0$ Hz, 6H, PMe), 7.2–7.8 (m, 10H, Ph). $^{13}C\{^1H\}$ NMR (CD_2Cl_2, -50 °C) δ -2.4 (dd, $^3J_{PC} = 11$ and 4 Hz, $^2J_{PtC} = 70$ Hz, $^1J_{SnC} = 187$ Hz, SnMe), 8.1 (dd, $^3J_{PC} = 10$ and 6 Hz, $^2J_{PtC} = 70$ Hz, GeMe), 17.9 (dd, $^1J_{PC} = 28$ Hz, $^3J_{PC} = 5$ Hz, $^2J_{PtC} = 37$ Hz, PMe), 18.9 (dd, $^1J_{PC} = 28$ Hz, $^3J_{PC} = 5$ Hz, $^2J_{PtC} = 33$ Hz, PMe), 127.9 (d, $^3J_{PC} = 1$ Hz, PPh), 128.0 (s, PPh), 129.6 (s, PPh), 129.7 (s, PPh), 131.2 (d, $^2J_{PC} = 12$ Hz, $^3J_{PtC} = 16$ Hz, PPh), 131.3 (d, $^2J_{PC} = 9$ Hz, $^3J_{PtC} = 18$ Hz, PPh), 138.4 (dd, $^1J_{PC} = 39$ Hz, $^3J_{PC} = 5$ Hz, PPh), 138.7 (dd, $^1J_{PC} = 38$ Hz, $^3J_{PC} = 3$ Hz, PPh). $^{31}P\{^1H\}$ NMR (CD_2Cl_2, -50 °C) δ -5.9 (d, $^2J_{PP} = 25$ Hz, $^1J_{PtP} = 2309$ Hz, $^2J_{^{119}SnP} = 1686$ Hz, $^2J_{^{117}SnP} = 1612$ Hz), -7.1 (d, $^2J_{PP} = 25$ Hz, $^1J_{PtP} = 1940$ Hz, $^2J_{^{119}SnP} = 189$ Hz, $^2J_{^{117}SnP} = 181$ Hz). Anal. Calcd for

Table 2. Site-Selectivities for the Insertion of Phenylacetylene into Platinum–Element Bonds

Complex	Site-selectivity	
	Kinetic condition	Thermodynamic condition
cis-[$Pt(SiMe_3)(SnMe_3)(PMe_2Ph)_2$]	Pt–Si:Pt–Sn = 100:0	Pt–Si:Pt–Sn = 100:0
cis-[$Pt(GeMe_3)(SnMe_3)(PMe_2Ph)_2$]	Pt–Ge:Pt–Sn = 20:80	Pt–Ge:Pt–Sn = 100:0

$C_{22}H_{40}GeP_2PtSn$: C, 35.10; H, 5.36%. Found: C, 35.20; H, 5.09%.

***trans*-1**. ^{1}H NMR (CD_2Cl_2, −50 °C) δ −0.37 (s, $^3J_{PtH}$ = 3.9 Hz, $^2J_{SnH}$ = 31.5 Hz, 9H, SnMe), −0.10 (s, $^3J_{PtH}$ = 11.4 Hz, 9H, GeMe), 1.95 (virtual triplet, J_{app} = 3.0 Hz, $^3J_{PtH}$ = 34.2 Hz, 12H, PMe), 7.2–7.8 (m, 10H, Ph). ^{31}P{^{1}H} NMR (CD_2Cl_2, −50 °C) δ −3.2 (s, $^1J_{PtP}$ = 2691 Hz, $^2J_{^{119}SnP}$ = 180 Hz, $^2J_{^{117}SnP}$ = 171 Hz).

Identification of *cis*-[Pt(GeMe$_3$){C(Ph)=CH(SnMe$_3$)}(PMe$_2$Ph)$_2$] (2a). Since **2a** is readily converted to **3a** in solution, its formation was confirmed by NMR spectroscopy without isolation. The sample solution was prepared by the treatment of **1** (48 mg, 64 μmol) with phenylacetylene (7.0 mg, 69 μmol) in CD_2Cl_2 (0.6 mL) in the presence of PMe_2Ph (1.0 mg, 7.2 μmol) at room temperature. Complex **1** disappeared within 3 h, as confirmed by ^{31}P{^{1}H} NMR spectroscopy, and the insertion complexes **2a** and **3a** were observed in an 80:20 ratio. Complex **2b** was similarly generated from *p*-$MeC_6H_4C{\equiv}CH$ instead of $PhC{\equiv}CH$ and identified.

2a. ^{1}H NMR (CD_2Cl_2, 20 °C) δ 0.09 (d, $^4J_{PH}$ = 1.7 Hz, $^3J_{PtH}$ = 16.1 Hz, 9H, GeMe), 0.31 (s, $^2J_{^{119}SnH}$ = 52.6 Hz, $^2J_{^{117}SnH}$ = 50.2 Hz, 9H, SnMe), 1.12 (d, $^2J_{PH}$ = 8.2 Hz, $^3J_{PtH}$ = 21.2 Hz, 3H, PMe), 1.32 (d, $^2J_{PH}$ = 8.1 Hz, $^3J_{PtH}$ = 19.8 Hz, 3H, PMe), 1.38 (d, $^2J_{PH}$ = 7.9 Hz, $^3J_{PtH}$ = 19.8 Hz, 3H, PMe), 1.62 (d, $^2J_{PH}$ = 11.7 Hz, $^3J_{PtH}$ = 23.4 Hz, 3H, PMe), 7.0–7.8 (m, 15H, Ph), 7.97 (dd, $^4J_{PH}$ = 19.6 and 4.0 Hz, $^3J_{PtH}$ = 106.6 Hz, 1H, PtC=C*H*). ^{13}C{^{1}H} NMR (CD_2Cl_2, 20 °C) δ −7.0 (s, $^1J_{^{119}SnC}$ = 327 Hz, $^1J_{^{117}SnC}$ = 312 Hz, SnMe), 6.0 (dd, $^3J_{PC}$ = 10 and 3 Hz, $^2J_{PtC}$ = 84 Hz, GeMe), 13.9 (dd, $^1J_{PC}$ = 24 Hz, $^3J_{PC}$ = 2 Hz, $^2J_{PtC}$ = 25 Hz, PMe), 14.8 (dd, $^1J_{PC}$ = 28 Hz, $^3J_{PC}$ = 2 Hz, $^2J_{PtC}$ = 33 Hz, PMe), 17.9 (dd, $^1J_{PC}$ = 29 Hz, $^3J_{PC}$ = 5 Hz, $^2J_{PtC}$ = 22 Hz, PMe), 18.4 (dd, $^1J_{PC}$ = 30 Hz, $^3J_{PC}$ = 5 Hz, $^2J_{PtC}$ = 38 Hz, PMe), 125.6 (s, $^5J_{PtC}$ = 6 Hz, Ph), 127.7 (s, Ph), 128.5 (s, PPh), 128.6 (s, PPh), 129.2 (d, $^4J_{PC}$ = 2 Hz, $^3J_{PtC}$ = 43 Hz, Ph), 129.8 (br(s), PPh), 130.8 (d, $^2J_{PC}$ = 12 Hz, $^3J_{PtC}$ = 12 Hz, PPh), 131.2 (d, $^2J_{PC}$ = 11 Hz, $^3J_{PtC}$ = 16 Hz, PPh), 138.3 (dd, $^1J_{PC}$ = 35 Hz, $^3J_{PC}$ = 2 Hz, PPh), 138.9 (dd, $^1J_{PC}$ = 39 Hz, $^3J_{PC}$ = 3 Hz, PPh), 152.6 (dd, $^3J_{PC}$ = 7 and 2 Hz, PtC(*Ph*)=CH), 179.4 (dd, $^2J_{PC}$ = 103 and 14 Hz, $^1J_{PtC}$ = 749 Hz, Pt*C*=CH). ^{31}P{^{1}H} NMR (CD_2Cl_2, 20 °C) δ −13.1 (d, $^2J_{PP}$ = 17 Hz, $^1J_{PtP}$ = 1729 Hz, $^4J_{SnP}$ = 29 Hz), −14.9 (d, $^2J_{PP}$ = 17 Hz, $^1J_{PtP}$ = 1842 Hz, $^4J_{SnP}$ = 68 Hz).

2b. ^{1}H NMR (CD_2Cl_2, 20 °C) δ 0.07 (d, $^4J_{PH}$ = 1.7 Hz, $^3J_{PtH}$ = 16.1 Hz, 9H, GeMe), 0.29 (s, $^2J_{^{119}SnH}$ = 52.6 Hz, $^2J_{^{117}SnH}$ = 50.2 Hz, 9H, SnMe), 1.12 (d, $^2J_{PH}$ = 8.2 Hz, $^3J_{PtH}$ = 21.4 Hz, 3H, PMe), 1.31 (d, $^2J_{PH}$ = 7.9 Hz, $^3J_{PtH}$ = 19.8 Hz, 3H, PMe), 1.38 (d, $^2J_{PH}$ = 7.9 Hz, $^3J_{PtH}$ = 19.8 Hz, 3H, PMe), 1.61 (d, $^2J_{PH}$ = 7.9 Hz, $^3J_{PtH}$ = 23.4 Hz, 3H, PMe), 2.36 (s, 3H, *p*-Me), 7.0–7.8 (m, 15H, Ph), 7.73 (dd, $^4J_{PH}$ = 19.8 and 3.8 Hz, $^3J_{PtH}$ = 128.2 Hz, 1H, PtC=C*H*). ^{13}C{^{1}H} NMR (CD_2Cl_2, 20 °C) δ −7.0 (s, $^1J_{SnC}$ = 326 Hz, SnMe), 6.0 (dd, $^3J_{PC}$ = 9 and 3 Hz, $^2J_{PtC}$ = 76 Hz, GeMe), 13.8 (dd, $^1J_{PC}$ = 25 Hz, $^3J_{PC}$ = 2 Hz, $^2J_{PtC}$ = 25 Hz, PMe), 14.8 (dd, $^1J_{PC}$ = 29 Hz, $^3J_{PC}$ = 3 Hz, $^2J_{PtC}$ = 29 Hz, PMe), 17.9 (dd, $^1J_{PC}$ = 28 Hz, $^3J_{PC}$ = 5 Hz, $^2J_{PtC}$ = 22 Hz, PMe), 18.4 (dd, $^1J_{PC}$ = 30 Hz, $^3J_{PC}$ = 5 Hz, $^2J_{PtC}$ = 38 Hz, PMe), 21.9 (s, *p*-Me), 128.2 (s, Ph), 128.4 (s, PPh), 128.5 (s, PPh), 128.8 (d, $^4J_{PC}$ = 2 Hz, $^3J_{PtC}$ = 44 Hz, Ph), 129.7 (br(s), PPh), 130.8 (d, $^2J_{PC}$ = 12 Hz, $^3J_{PtC}$ = 12 Hz, PPh), 131.3 (d, $^2J_{PC}$ = 12 Hz, $^3J_{PtC}$ = 17 Hz, PPh), 135.2 (s, $^5J_{PtC}$ = 7 Hz, Ph), 138.4 (dd, $^1J_{PC}$ = 35 Hz, $^3J_{PC}$ = 1 Hz, PPh), 138.9 (dd, $^1J_{PC}$ = 39 Hz, $^3J_{PC}$ = 3 Hz, PPh), 149.8 (dd, $^3J_{PC}$ = 7 and 2 Hz, PtC(*Ph*)=CH), 178.9 (dd, $^2J_{PC}$ = 103 and 14 Hz, Pt*C*=CH). ^{31}P{^{1}H} NMR (CD_2Cl_2, 20 °C) δ −13.0 (d, $^2J_{PP}$ = 16 Hz, $^1J_{PtP}$ = 1717 Hz, $^4J_{SnP}$ = 22 Hz), −14.9 (d, $^2J_{PP}$ = 18 Hz, $^1J_{PtP}$ = 1868 Hz, $^4J_{SnP}$ = 64 Hz).

Preparation of *cis*-[Pt{C(Ph)=CH(GeMe$_3$)}(SnMe$_3$)(PMe$_2$Ph)$_2$] (3a). To a solution of *cis*-**1** (162 mg, 0.22 mmol) in CH_2Cl_2 (5 mL) was added phenylacetylene (43 mg, 0.42 mmol) at room temperature. The starting **1** disappeared in 2 h, and selective formation of **3a** was observed by ^{31}P{^{1}H} NMR spectroscopy. Solvent was removed by pumping, and the resulting pale yellow residue was dried under vacuum. This product was dissolved in Et_2O (ca. 0.5 mL) at −78 °C. Pentane (1 mL) was added, and the mixture was vigorously stirred at the same temperature to give white precipitation of **3a**, which was collected by filtration, washed with pentane (1 mL × 2), and dried under vacuum (132 mg, 70%). Recrystallization of this crude product from Et_2O/pentane gave colorless crystals of **3a** (106 mg, 56%). Complex **3b** was similarly prepared in 67% yield.

3a. ^{1}H NMR (CD_2Cl_2, 20 °C) δ −0.15 (d, $^4J_{PH}$ = 0.7 Hz, $^3J_{PtH}$ = 7.8 Hz, $^2J_{SnH}$ = 37.5 Hz, 9H, SnMe), 0.38 (s, 9H, GeMe), 1.14 (d, $^2J_{PH}$ = 8.4 Hz, $^3J_{PtH}$ = 24.9 Hz, 3H, PMe), 1.35 (d, $^2J_{PH}$ = 8.1 Hz, $^3J_{PtH}$ = 23.4 Hz, 3H, PMe), 1.43 (d, $^2J_{PH}$ = 7.8 Hz, $^3J_{PtH}$ = 22.2 Hz, 3H, PMe), 1.61 (d, $^2J_{PH}$ = 8.1 Hz, $^3J_{PtH}$ = 26.1 Hz, 3H, PMe), 7.0–7.8 (m, 15H, Ph), 7.60 (dd, $^4J_{PH}$ = 19.5 and 4.5 Hz, $^3J_{PtH}$ = 112.2 Hz, 1H, PtC=C*H*). ^{13}C{^{1}H} NMR (CD_2Cl_2, 20 °C) δ −4.3 (dd, $^3J_{PC}$ = 10 and 2 Hz, $^2J_{PtC}$ = 78 Hz, $^1J_{^{119}SnC}$ = 193 Hz, $^1J_{^{117}SnC}$ = 182 Hz, SnMe), 0.47 (s, GeMe), 13.7 (dd, $^1J_{PC}$ = 27 Hz, $^3J_{PC}$ = 2 Hz, $^2J_{PtC}$ = 29 Hz, PMe), 14.5 (dd, $^1J_{PC}$ = 29 Hz, $^3J_{PC}$ = 3 Hz, $^2J_{PtC}$ = 39 Hz, PMe), 18.8 (dd, $^1J_{PC}$ = 30 Hz, $^3J_{PC}$ = 5 Hz, $^2J_{PtC}$ = 29 Hz, PMe), 19.5 (dd, $^1J_{PC}$ = 32 Hz, $^3J_{PC}$ = 5 Hz, $^2J_{PtC}$ = 41 Hz, PMe), 125.7 (s, $^5J_{PtC}$ = 6 Hz, Ph), 127.6 (s, Ph), 128.4 (s, PPh), 128.5 (s, PPh), 129.0 (d, $^4J_{PC}$ = 2 Hz, $^3J_{PtC}$ = 45 Hz, Ph), 129.7 (br(s), PPh), 130.9 (d, $^2J_{PC}$ = 12 Hz, $^3J_{PtC}$ = 17 Hz, PPh), 131.0 (d, $^2J_{PC}$ = 12 Hz, $^3J_{PtC}$ = 17 Hz, PPh), 132.8 (dd, $^3J_{PC}$ = 8 and 5 Hz, $^2J_{PtC}$ = 47 Hz, PtC=*C*H), 138.1 (dd, $^1J_{PC}$ = 36 Hz, $^3J_{PC}$ = 2 Hz, $^2J_{PtC}$ = 17 Hz, PPh), 139.0 (dd, $^1J_{PC}$ = 43 Hz, $^3J_{PC}$ = 3 Hz, $^2J_{PtC}$ = 17 Hz, PPh), 153.2 (dd, $^3J_{PC}$ = 6 and 2 Hz, PtC(*Ph*)=CH), 172.7 (dd, $^2J_{PC}$ = 100 and 13 Hz, $^1J_{PtC}$ = 704 Hz, Pt*C*=CH). ^{31}P{^{1}H} NMR (CD_2Cl_2, 20 °C) δ −13.8 (d, $^2J_{PP}$ = 16 Hz, $^1J_{PtP}$ = 2067 Hz, $^2J_{^{119}SnP}$ = 1789 Hz, $^2J_{^{117}SnP}$ = 1710 Hz), −16.0 (d, $^2J_{PP}$ = 16 Hz, $^1J_{PtP}$ = 1938 Hz, $^2J_{^{119}SnP}$ = 168 Hz, $^2J_{^{117}SnP}$ = 160 Hz). Anal. for $C_{30}H_{46}GeP_2PtSn$: C, 42.14; H, 5.42%. Found: C, 42.53; H 5.27%.

3b. ^{1}H NMR (CD_2Cl_2, 20 °C) δ −0.14 (d, $^4J_{PH}$ = 0.7 Hz, $^3J_{PtH}$ = 7.7 Hz, $^2J_{SnH}$ = 37.5 Hz, 9H, SnMe), 0.39 (s, 9H, GeMe), 1.15 (d, $^2J_{PH}$ = 8.8 Hz, $^3J_{PtH}$ = 25.1 Hz, 3H, PMe), 1.35 (d, $^2J_{PH}$ = 8.3 Hz, $^3J_{PtH}$ = 23.4 Hz, 3H, PMe), 1.44 (d, $^2J_{PH}$ = 7.9 Hz, $^3J_{PtH}$ = 22.3 Hz, 3H, PMe), 1.62 (d, $^2J_{PH}$ = 7.9 Hz, $^3J_{PtH}$ = 21.2 Hz, 3H, PMe), 2.32 (s, 3H, *p*-Me), 7.0–7.7 (m, 15H, Ph and PtC=C*H*). ^{13}C{^{1}H} NMR (CD_2Cl_2, 20 °C) δ −4.3 (dd, $^3J_{PC}$ = 9 and 2 Hz, $^2J_{PtC}$ = 78 Hz, $^1J_{SnC}$ = 189 Hz, SnMe), 0.48 (s, GeMe), 13.6 (dd, $^1J_{PC}$ = 27 Hz, $^3J_{PC}$ = 2 Hz, $^2J_{PtC}$ = 29 Hz, PMe), 14.5 (dd, $^1J_{PC}$ = 29 Hz, $^3J_{PC}$ = 3 Hz, $^2J_{PtC}$ = 39 Hz, PMe), 18.7 (dd, $^1J_{PC}$ = 30 Hz, $^3J_{PC}$ = 5 Hz, $^2J_{PtC}$ = 28 Hz, PMe), 19.4 (dd, $^1J_{PC}$ = 31 Hz, $^3J_{PC}$ = 5 Hz, $^2J_{PtC}$ = 43 Hz, PMe), 21.1 (s, *p*-Me), 128.3 (s, PPh), 128.4 (s, PPh), 128.5 (s, Ph), 129.0 (d, $^4J_{PC}$ = 2 Hz, $^3J_{PtC}$ = 45 Hz, Ph), 129.6 (br(s), PPh), 130.8 (d, $^2J_{PC}$ = 12 Hz, $^3J_{PtC}$ = 14 Hz, PPh), 131.0 (d, $^2J_{PC}$ = 11 Hz, $^3J_{PtC}$ = 17 Hz, PPh), 131.5 (t, $^3J_{PC}$ = 6 Hz, $^2J_{PtC}$ = 47 Hz, PtC=*C*H), 135.2 (s, Ph), 138.2 (dd, $^1J_{PC}$ = 36 Hz, $^3J_{PC}$ = 3 Hz), 139.1 (dd, $^1J_{PC}$ = 42 Hz, $^3J_{PC}$ = 3 Hz, $^2J_{PtC}$ = 16 Hz, PPh), 153.2 (dd, $^3J_{PC}$ = 5 and 2 Hz, $^2J_{PtC}$ = 16 Hz, PtC(*Ph*)=CH), 172.3 (dd, $^2J_{PC}$ = 100 and 13 Hz, $^1J_{PtC}$ = 698 Hz, Pt*C*=CH). ^{31}P{^{1}H} NMR (CD_2Cl_2, 20 °C) δ −13.7 (d, $^2J_{PP}$ = 18 Hz, $^1J_{PtP}$ = 2076 Hz, $^2J_{^{119}SnP}$ = 1795 Hz, $^2J_{^{117}SnP}$ = 1713 Hz), −16.2 (d, $^2J_{PP}$ = 16 Hz, $^1J_{PtP}$ = 1930 Hz, $^2J_{^{119}SnP}$ =

Table 3. Crystallographic Data and Details of Structure Determination for *cis*-**1** and **3a**

	cis-**1**	**3a**
Formula	$C_{22}H_{40}GeP_2PtSn$	$C_{30}H_{46}GeP_2PtSn$
Formula weight	752.88	855.01
Crystal appearance	Yellow plate	Colorless block
Crystal size/mm	$0.38 \times 0.25 \times 0.06$	$0.35 \times 0.15 \times 0.04$
Crystal system	orthorhombic	triclinic
Space group	*Pbca* (#61)	$P\bar{1}$ (#2)
a/Å	15.306(2)	10.544(1)
b/Å	17.511(2)	11.196(1)
c/Å	19.724(3)	15.506(2)
α/deg		88.191(9)
β/deg		80.600(8)
γ/deg		66.451(7)
V/Å^3	5286(1)	1654.3(4)
Z	8	2
d_{calcd}/g cm^{-3}	1.892	1.716
μ(Mo Kα)/cm^{-1}	74.52	59.65
Temp/°C	−70	−50
$2\theta_{max}$/deg	55.0	55.0
No. of reflections collected	52199	16291
No. of unique reflections	6054 ($R_{int} = 0.123$)	7431 ($R_{int} = 0.030$)
Absorption correction	Numerical	Empirical
Transmission factors	0.2137–0.7532	0.5639–0.7877
No. of observed reflections	5685 ($I \geq 2.0\sigma(I)$)	6839 ($I \geq 2.0\sigma(I)$)
No. of variables	244	316
R[a)] ($I \geq 2\sigma(I)$)	0.082	0.044
R_w[b)] (all data)	0.213	0.107
GOF	1.16	1.07
Max and min peak/e Å^{-3}	4.69, −2.94 (near Pt)	1.75, −2.29 (near Pt)

a) $R = \Sigma||F_o| - |F_c||/\Sigma|F_o|$. b) $R_w = [\Sigma w(F_o^2 - F_c^2)^2/\Sigma w(F_o^2)^2]^{1/2}$.

168 Hz, $^2J_{^{117}SnP} = 160$ Hz). Anal. for $C_{31}H_{48}GeP_2PtSn$: C, 42.85; H, 5.57%. Found: C, 42.83; H, 5.37%.

Preparation of *cis*-[Pt(GeMe$_3$){C(CO$_2$Me)=C(CO$_2$Me)-(SnMe$_3$)}(PMe$_2$Ph)$_2$] (2c). To a solution of **1** (182 mg, 0.24 mmol) in CH_2Cl_2 (5 mL) was added dimethyl acetylenedicarboxylate (42 mg, 0.30 mmol) at −50 °C. The color of the solution changed instantly from yellow to red. The solvent was removed by pumping at room temperature, and the resulting red oily material was dissolved in Et_2O (0.5 mL) at −78 °C. The addition of pentane (1 mL) with stirring led to the precipitation of a reddish orange solid, which was collected by filtration, washed with pentane (1 mL × 2) at −78 °C, and dried under vacuum (175 mg, 81% yield).

2c. ^{1}H NMR (CD_2Cl_2, 20 °C) δ 0.13 (d, $^4J_{PH} = 1.8$ Hz, $^3J_{PtH} = 14.7$ Hz, 9H, GeMe), 0.34 (s, $^2J_{^{119}SnH} = 53.7$ Hz, $^2J_{^{117}SnH} = 51.6$ Hz, 9H, SnMe), 1.25 (d, $^2J_{PH} = 8.3$ Hz, $^3J_{PtH} = 23.1$ Hz, 3H, PMe), 1.48 (d, $^2J_{PH} = 9.8$ Hz, $^3J_{PtH} = 19.8$ Hz, 3H, PMe), 1.51 (d, $^2J_{PH} = 9.4$ Hz, $^3J_{PtH} = 15.6$ Hz, 3H, PMe), 1.57 (d, $^2J_{PH} = 9.4$ Hz, $^3J_{PtH} = 26.0$ Hz, 3H, PMe), 3.59 (s, 3H, CO_2Me), 3.66 (s, 3H, CO_2Me), 7.2–7.8 (m, 10H, Ph). ^{13}C{^{1}H} NMR (CD_2Cl_2, 20 °C) δ −6.4 (s, $^1J_{^{119}SnC} = 352$ Hz, $^1J_{^{117}SnC} = 336$ Hz, SnMe), 5.4 (dd, $^3J_{PC} = 8$ and 3 Hz, $^2J_{PtC} = 64$ Hz, GeMe), 13.4 (d, $^1J_{PC} = 28$ Hz, $^2J_{PtC} = 26$ Hz, PMe), 16.2 (dd, $^1J_{PC} = 29$ Hz, $^3J_{PC} = 3$ Hz, $^2J_{PtC} = 30$ Hz, PMe), 16.8 (dd, $^1J_{PC} = 31$ Hz, $^3J_{PC} = 4$ Hz, $^2J_{PtC} = 32$ Hz, PMe), 18.2 (dd, $^1J_{PC} = 33$ Hz, $^3J_{PC} = 5$ Hz, $^2J_{PtC} = 32$ Hz, PMe), 50.6 (s, CO_2Me), 51.3 (s, CO_2Me), 128.4 (d, $^3J_{PC} = 10$ Hz, PPh), 128.7 (d, $^3J_{PC} = 10$ Hz, PPh), 129.9 (d, $^4J_{PC} = 2$ Hz, PPh), 130.0 (d, $^4J_{PC} = 3$ Hz, PPh), 131.0 (d, $^2J_{PC} = 10$ Hz, $^3J_{PtC} = 17$ Hz, PPh), 131.2 (d, $^2J_{PC} = 7$ Hz, $^3J_{PtC} = 17$ Hz, PPh), 132.9 (t, $^3J_{PC} = 5$ Hz, PtC=*C*), 137.6 (dd, $^1J_{PC} = 47$ Hz, $^3J_{PC} = 5$ Hz, PPh), 137.8 (dd, $^1J_{PC} = 35$ Hz, $^3J_{PC} = 1$ Hz, PPh), 168.4 (dd, $^3J_{PC} = 13$ and 3 Hz, PtC(*C*O$_2$Me)=C), 177.1 (d, $^4J_{PC} = 5$ Hz, PtC=C(*C*O$_2$Me)), 193.9 (dd, $^2J_{PC} = 100$ and 13 Hz, Pt*C*=C). ^{31}P{^{1}H} NMR (CD_2Cl_2, 20 °C) δ −11.8 (d, $^2J_{PP} = 21$ Hz, $^1J_{PtP} = 1678$ Hz, $^4J_{SnP} = 27$ Hz), −15.7 (d, $^2J_{PP} = 21$ Hz, $^1J_{PtP} = 2174$ Hz, $^4J_{SnP} = 41$ Hz). Anal. for $C_{28}H_{46}GeO_4P_2PtSn$: C, 37.58; H, 5.18%. Found: C, 37.67; H, 5.16%.

Reaction of 1 with Phenylacetylene (Fig. 3 and Table 1). A typical procedure is reported for the experiment given in Fig. 3b. Complex *cis*-**1** (11.3 mg, 15.0 μmol) was placed in an NMR sample tube equipped with a rubber septum cap and dissolved in CD_2Cl_2 (0.6 mL). PMe_2Ph (9 mM) was added at room temperature, and the sample was cooled to −78 °C. Phenylacetylene (15.3 mg, 0.15 mmol) was added, and the sample tube was placed in an NMR sample probe controlled at 20.0 ± 0.1 °C. The amounts of *cis*-**1**, *trans*-**1**, **2a**, and **3a** at time t were determined by the peak integration of the following singlet signals: *cis*-**1**, δ 0.29 (s, $GeMe_3$); *trans*-**1**, δ −0.24 (s, $SnMe_3$); **2a**, δ 0.31 (s, $SnMe_3$); **3a**: δ 0.38 (s, $GeMe_3$).

Isomerization of 2a to 3a (Cross-over Experiments). Complex **1** (11.3 mg, 15.0 μmol) was dissolved in toluene-d_8 (0.6 mL) containing free PMe_2Ph (2.5 mM) at room temperature. Phenylacetylene (1.5 mg, 14.7 μmol) was added, and the sample solution was allowed to stand for 3 h at room temperature. ^{1}H NMR analysis revealed the formation of **2a** and **3a** in an 80:20 ratio. Then, *p*-$MeC_6H_4C{\equiv}CH$ (5.6 mL, 44.8 μmol) was added, and the sample was warmed at 50 °C for 12 h. The ^{1}H NMR spectrum measured at 20 °C showed the complete conversion of **2a** to **3a**; no trace

of the methyl proton signal of **3b** at δ 2.20 was detected. A similar experiment was carried out using PhC≡CH (5.0 mL, 0.46 mmol) and a 77:23 ratio mixture of **2b** and **3b**. In this case, no trace of the methyl proton signal of *p*-$MeC_6H_4C{\equiv}CH$ at δ 1.96 was detected after the isomerization of **2b** to **3b**.

X-ray Structural Analysis. X-ray diffraction studies of *cis*-**1** and **3a** were made on a Rigaku/MSC Mercury CCD diffractometer with graphite monochromated Mo Kα radiation ($\lambda = 0.71070$ Å (1 Å $= 1 \times 10^{-10}$ m)). The intensity data were collected at -70 (*cis*-**1**) and -50 °C (**3a**), and corrected for Lorentz and polarization effects and absorption (NUMABS and REQAB, respectively). All calculations were performed with the teXsan crystallographic software package of Molecular Structure Corporation. The structure was solved by heavy atom Patterson methods (PATTY and SAP91), and expanded using Fourier techniques (DIRDIF94).[16,17] All non-hydrogen atoms were refined anisotropically (SHELXL-97).[18] In the final cycles of refinement, hydrogen atoms were located at idealized positions (d(C–H) = 0.95 Å) with isotropic temperature factors ($B_{iso} = 1.20B_{bonded\ atom}$) and were included in calculation without refinement of their parameters.

Crystallographic data and details of data collection and refinement are summarized in Table 3. The data have been deposited at the CCDC, 12 Union Road, Cambridge CB2 1EZ, UK and copies can be obtained on request, free of charge, by quoting the publication citation and the deposition numbers CCDC 236892 and 236893.

References

1 For reviews, see: a) I. Beletskaya and C. Moberg, *Chem. Rev.*, **99**, 3435 (1999). b) M. Suginome and Y. Ito, *Chem. Rev.*, **100**, 3221 (2000). c) H. K. Sharma and K. H. Pannell, *Chem. Rev.*, **95**, 1351 (1995). d) U. Schubert, *Angew. Chem., Int. Ed.*, **33**, 419 (1994). e) C. A. Recatto, *Aldrichimica Acta*, **95**, 1351 (1995).

2 For theoretical studies, see: Si–Si: a) S. Sakaki, N. Mizoe, and M. Sugimoto, *Organometallics*, **17**, 2510 (1998). b) S. Sakaki, M. Ogawa, and Y. Musashi, *J. Organomet. Chem.*, **535**, 25 (1997). c) S. Sakaki, M. Ogawa, and M. Kinoshita, *J. Phys. Chem.*, **99**, 9933 (1995). d) S. Sakaki, M. Ogawa, Y. Musashi, and T. Arai, *J. Am. Chem. Soc.*, **116**, 7258 (1994). e) A. Bottoni, A. P. Higueruelo, and G. P. Miscione, *J. Am. Chem. Soc.*, **124**, 5506 (2002). f) S.-Y. Kang, T. Yamabe, A. Naka, M. Ishikawa, and K. Yoshizawa, *Organometallics*, **21**, 150 (2002). Si–Sn: g) M. Hada, Y. Tanaka, M. Ito, M. Murakami, H. Amii, Y. Ito, and H. Nakatsuji, *J. Am. Chem. Soc.*, **116**, 8754 (1994).

3 H. Yamashita, T.-a. Kobayashi, M. Tanaka, J. A. Samuels, and W. E. Streib, *Organometallics*, **11**, 2330 (1992).

4 Y.-J. Kim, J.-I. Park, S.-C. Lee, K. Osakada, M. Tanabe, J.-C. Choi, T. Koizumi, and T. Yamamoto, *Organometallics*, **18**, 1349 (1999).

5 a) Y. Obora, Y. Tsuji, K. Nishiyama, M. Ebihara, and T. Kawamura, *J. Am. Chem. Soc.*, **118**, 10922 (1996). b) Y. Tsuji, K. Nishiyama, S. Hori, M. Ebihara, and T. Kawamura, *Organometallics*, **17**, 507 (1998). c) Y. Tsuji and Y. Obora, *J. Organomet. Chem.*, **611**, 343 (2000).

6 K. Mochida, T. Wada, K. Suzuki, W. Hatanaka, Y. Nishiyama, M. Nanjo, A. Sekine, Y. Ohashi, M. Sakamoto, and A. Yamamoto, *Bull. Chem. Soc. Jpn.*, **74**, 123 (2001).

7 a) F. Ozawa, *J. Organomet. Chem.*, **611**, 332 (2000). b) T. Sagawa, Y. Sakamoto, R. Tanaka, H. Katayama, and F. Ozawa, *Organometallics*, **22**, 4433 (2003). c) F. Ozawa, Y. Sakamoto, T. Sagawa, R. Tanaka, and H. Katayama, *Chem. Lett.*, **1999**, 1307. d) F. Ozawa and J. Kamite, *Organometallics*, **17**, 5630 (1998). e) F. Ozawa and T. Hikida, *Organometallics*, **15**, 4501 (1996). f) T. Hikida, K. Onitsuka, K. Sonogashira, T. Hayashi, and F. Ozawa, *Chem. Lett.*, **1995**, 985. g) T. Sagawa, Y. Asano, and F. Ozawa, *Organometallics*, **21**, 5879 (2002).

8 a) F. Ozawa, T. Hikida, and T. Hayashi, *J. Am. Chem. Soc.*, **116**, 2844 (1994). b) F. Ozawa, T. Hikida, K. Hasebe, and T. Mori, *Organometallics*, **17**, 1018 (1998). c) F. Ozawa, M. Kitaguchi, and H. Katayama, *Chem. Lett.*, **1999**, 1289. d) K. Hasebe, J. Kamite, T. Mori, H. Katayama, and F. Ozawa, *Organometallics*, **19**, 2022 (2000). e) F. Ozawa and T. Mori, *Organometallics*, **22**, 3593 (2003). f) F. Ozawa, M. Sugawara, and T. Hayashi, *Organometallics*, **13**, 3237 (1994). g) F. Ozawa, M. Sugawara, K. Hasebe, and T. Hayashi, *Inorg. Chim. Acta*, **296**, 19 (1999).

9 Y.-J. Kim, E.-H. Choi, and S.-W. Lee, *Organometallics*, **22**, 3316 (2003), and references cited therein.

10 For catalytic addition of germylstannanes to alkynes, see: a) E. Piers and R. T. Skerlj, *J. Chem. Soc., Chem. Commun.*, **1987**, 1025. b) T. N. Mitchell, U. Schneider, and B. Frohling, *J. Organomet. Chem.*, **384**, C53 (1990). c) T. Nakano, Y. Senda, and T. Miyamoto, *Chem. Lett.*, **2000**, 1408. d) Y. Senda, Y.-i. Oguchi, M. Terayama, T. Asai, T. Nakano, and T. Migita, *J. Organomet. Chem.*, **622**, 302 (2001).

11 H. S. Gutowsky and C. H. Holm, *J. Chem. Phys.*, **25**, 1228 (1956).

12 C. J. Levy and R. J. Puddephatt, *J. Am. Chem. Soc.*, **119**, 10127 (1997).

13 a) R. Walsh, "The Chemsitry of Organic Silicon Compounds, Part 1," ed by S. Patai and Z. Rappoport, John Wiley & Sons, Chichester (1989), p. 371. b) G. Pilcher and H. A. Skinner, "The Chemsitry of Metal–Carbon Bond, Vol. 1," ed by F. R. Hartley and S. Patai, John Wiley & Sons, Chichester (1982), p. 43.

14 The silyl(germyl) complex could not be prepared in spite of several trials.

15 L. E. Crascall and J. L. Spencer, *Inorg. Synth.*, **28**, 126 (1990).

16 PATTY and DIRDIF94: P. T. Beurskens, G. Admiraal, G. Beurskens, W. P. Bosman, R. de Gelder, R. Israel, and J. M. M. Smits, "The DIRDIF-94 Program System," Technical Report of the Crystallography Laboratory, University of Nijmegen, The Netherlands (1994).

17 SAPI91: H.-F. Fan, "Structure Analysis Programs with Intelligent Control," Rigaku Corporation, Tokyo, Japan (1991).

18 SHELXL-97: G. M. Sheldrick, "Program for the Refinement of Crystal Structuers," University of Göettingen, Germany (1997).